Science of the Total Environment 572 (2016) 476–486

Contents lists available at ScienceDirect

Science of the Total Environment

journal homepage: www.elsevier.com/locate/scitotenv

Spatial scale effect on sediment dynamics in basin-wide floods within a typical agro-watershed: A case study in the hilly loess region of the Chinese Loess Plateau

Le-Tao Zhang [a,b], Zhan-Bin Li [a,c,*], Shan-Shan Wang [a,b]

[a] State Key Laboratory of Soil Erosion and Dryland Farming on the Loess Plateau, Institute of Soil and Water Conservation, Chinese Academy of Sciences and Ministry of Water Resources, Yangling, Shaanxi 712100, PR China
[b] University of Chinese Academy of Sciences, Beijing 100049, PR China
[c] Key Laboratory of Northwest Water Resources and Environment Ecology of Ministry of Education, Xi'an University of Technology, Xi'an, Shaanxi 710048, PR China

HIGHLIGHTS

- Spatial invariability of sediment delivery was illustrated in basin system.
- Intra- and inter-scale runoff–sediment relationships were analyzed in basin system.
- The great sediment-reducing potential of flood regulation was expounded.

GRAPHICAL ABSTRACT

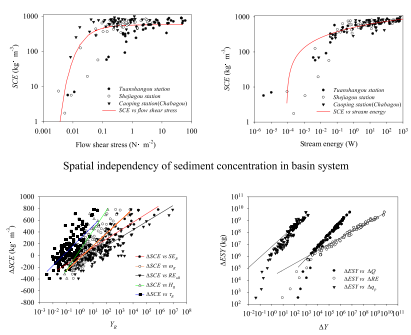

ARTICLE INFO

Article history:
Received 7 October 2015
Received in revised form 12 August 2016
Accepted 12 August 2016
Available online xxxx

Editor: D. Barcelo

Keywords:
Spatial independency
Flow–sediment relationship
Runoff regulation
Sediment control

ABSTRACT

Scale issues, which have been extensively studied in the domain of soil erosion, are considerably significant in geomorphologic processes and hydrologic modelling. However, relatively scarce efforts have been made to quantify the spatial scale effect on event-based sediment dynamics in basin-wide floods. To address this issue, sediment-runoff yield data of 44 basin-wide flood events were collected from gauging stations at the Chabagou river basin, a typical agro-basin (unmanaged) in the hilly loess region of the Chinese Loess Plateau. Thus, the spatial scale effect on event-based sediment dynamics was investigated in the basin system across three different spatial scales from sublateral to basin outlet. Results showed that the event-based suspended sediment concentration, as well as the intra- and inter-scale flow–sediment relationships remained spatially constant. Hence, almost all the sediment-laden flows can reach at the detachment-limited maximum concentration across scales, specifically for hyperconcentrated flows. Consequently, limited influence was exerted by upstream sediment-laden flow on downstream sediment output, particularly for major sediment-producing events. However, flood peak discharge instead of total flood runoff amount can better interpret the dynamics of sediment yield across scales. As a composite parameter, the proposed stream energy factor combines flood runoff depth and flood peak discharge, thereby showing more advantages to describe the event-based inter-scale flow–sediment relationship than other flow-related variables. Overall, this study demonstrates the process-specific characteristics of soil erosion by water flows in the basin system. Therefore, event-based sediment control should be

* Corresponding author at: State Key Laboratory of Soil Erosion and Dryland Farming on the Loess Plateau, Institute of Soil and Water Conservation, Chinese Academy of Sciences and Ministry of Water Resources, Yangling, Shaanxi 712100, PR China.
E-mail addresses: zhangletao10@mails.ucas.ac.cn (L.-T. Zhang), zbli@ms.iswc.ac.cn (Z.-B. Li).

http://dx.doi.org/10.1016/j.scitotenv.2016.08.082
0048-9697/© 2016 Published by Elsevier B.V.

oriented by the process to cut off the connectivity of hyperconcentrated flows and redistribute the erosive energy of flowing water in terms of temporality and spatiality. Furthermore, evaluation of soil conservation benefits should be based on the process of runoff regulation to comprehensively assess the efficiency of anti-erosion strategies in sediment control at the basin scale.

© 2016 Published by Elsevier B.V.

1. Introduction

Soil erosion is an integrated process linking interrelated subprocesses of dislodgement, detachment, transportation, and soil-particle deposition caused by erosive agents (Cerdà et al. 2013; Ellison 1948; Meyer and Wischmeier 1969). Therefore, factors disturbing any subprocess related with soil erosion may alter the rate and pattern of erosion, as well as those associated with consequent sediment behavior, affecting the total sediment export. As a basic driving force and medium for sediment delivery, surface runoff is generally associated with concentration, transmission, transformation, and degradation of flow energy and erosive power, which can cause soil detachment and sediment incipient motion, as well as sediment transportation and deposition at the watershed scale. Hence, runoff-related erosivity indices of various combinations demonstrated some advantages over other variables related to rainfall storm characteristics alone in sediment yield estimation at plots or watershed outlets (Bagarello et al. 2010; Foster et al. 1982; Kinnell 1997; Kinnell 2014; Williams and Berndt 1977; Zheng and Chen 2015). However, those erosivity indices are scale-based for site-specific sediment yield estimation, and their applicability may vary between erosion patterns and across sites of different spatial scales (Zheng and Chen 2015). Consequently, the feasibility of those erosivity indices in process-based sediment yield estimation and spatial scale-dependent assessment of sediment flow behavior still needs further investigation. Thus, a conceptual basis for sediment yield prediction will be consolidated through identification of spatial scale effect on sediment dynamics.

In recent years, the spatial behavior of sediment-laden flow has received increasing attention at multiple scales ranging from field microplot to catchment and river basin (Bautista et al. 2007; Boix-Fayos et al. 2006; de Vente et al. 2013; de Vente and Poesen 2005; Jetten et al. 2003; Xu and Yan 2005; Parsons et al. 2006) because of its irreplaceable significance in determining on-site soil detachment and off-site sediment delivery. Addressing this issue will benefit profound perception of soil erosion mechanisms, improved hazard assessment on soil erosion, promoted accuracy of extrapolation in sediment yield estimation, and proper design of anti-erosion strategies (Cerdà et al. 2013; Jetten et al. 1999; Parsons et al. 2004). The sediment concentration dynamics and flow–sediment relationships have been examined under different rainfall-storm types across varying spatial scales (de Vente et al. 2007; Fang et al. 2008; Fang et al., 2007a, b; Fang et al. 2011; Li et al. 2009; Zheng et al. 2008; Zheng et al. 2015; Zheng et al. 2011; Zheng et al. 2013; Zheng et al. 2012). These studies contributed to further recognition of the role of spatial scale in controlling dominant soil erosion process and erosion rates, up-scaling of sediment yield prediction, identification of sediment redistribution, and model establishment (Cammeraat 2004; de Vente et al. 2007; Favis-Mortlock et al. 2001; Kirkby et al. 1996; Mayor et al. 2011; Zheng et al. 2008; Rodríguez-Blanco et al. 2013; Zheng et al. 2012). Nevertheless, the spatial scale dependency of sediment dynamics is commonly studied through corresponding statistical analysis within single scales, followed by lateral comparison across multiple scales at day and annual time scales (Fang et al. 2008; Fang et al., 2007a, b; Zheng et al. 2015), regardless of the tempo-spatial consistence, specifically for basin-wide flood events. This limitation prevents further understanding of the spatial scale effect on event-based sediment dynamics within a basin system.

In a basin system, hydrological and geomorphological processes operating at different scale levels are related and connected to induce the development of soil erosion across scales (Belnap et al. 2005; Boix-Fayos et al. 2006; Cammeraat 2002), albeit markedly varied scale dependency of controlling processes of sediment movement in the downstream direction (de Vente and Poesen 2005; Osterkamp and Toy 1997; Puigdef Bregas 2005). This result highlights the systematic functions of scale interactions and feedback relationships between predominating processes in spatial heterogeneity development and basin system evolution, within and across different scale levels (Boix-Fayos et al. 2006; Cammeraat 2004; Cammeraat 2002; Peters and Havstad 2006). Certainly, small events at smaller scales can slowly make some differences in preparation for large processes at larger scales. Boix-Fayos et al. (2006) pointed out that events of higher frequencies contribute more to sediment export at the catchment scale on the inter-annual timescale because sediment transport in a basin system is more sensitive to the impetus of flow dynamics of the main channel stream than that of sediment source areas on hillslopes with gullies. However, both basin-wide and localized floods may occur at the basin scale because of the spatial heterogeneity of rainstorms and underlying hydrological conditions. Accordingly, flood hydrographs vary across scales. The scale-specific soil erosion processes are therefore driven by different erosive agents. Probably, not all the soil erosion processes operating at smaller scales upstream cause a difference to event-based sediment flow behavior at larger scales of downstream. Hence, basin-wide-based sediment-producing events, specifically driven by hyperconcentrated flows, should be selected to illuminate the spatial scale effect on event-based sediment dynamics within a basin system.

The hilly and gully region on the Chinese Loess Plateau is strongly prone to hyperconcentrated flows and high soil erosion rates (Xu 1999; Xu 2004). Many pluvial erosion events occurred because of distinct erosion environment, thereby providing sufficiently recorded data for runoff and sediment analysis on this region. Chabagou, a third-order tributary of the Yellow River, plays an important role in the studies of spatial scale effects on soil erosion process (Fang et al. 2008; Fang et al., 2007a, b; Fang et al. 2011; Zheng et al. 2008; Zheng et al. 2015; Zheng et al. 2011; Zheng et al. 2013; Zheng et al. 2012). Nested gauging stations and runoff plots of varying spatial scales were established for long-term hydrological observations, sediment measurement, and meteorological data collection within the basin. The present study aims to investigate the spatial scale effect on sediment dynamics in basin-wide floods at event time scale within the basin system from sub-basin to basin outlet. The specific objectives are as follows: (1) to examine the spatial behavior of the suspended sediment concentration dynamics across scales, (2) to quantify the intra- and inter-scale flow–sediment relationships, and (3) to determine the scale-specific contribution of upstream sediment-laden flow to the total sediment export downstream. This study may be referential for revealing the mechanism of soil erosion caused by hyperconcentrated flows and contribute to a further understanding of the functions of *anti*-erosion precautions in the sediment control of drainage basins.

2. Study area, data sources and treatments

2.1. Description of the study area

The Zizhou Runoff Experimental Station which was situated on Chabagou drainage basin in Zizhou County, Shannxi Province, was established in 1958 and closed in 1969. The Chabagou river (109° 47′

E, 37° 31′N), a first branch of Dalihe River, is located in the No.1 sub-region of the gullied rolling loess plateau. The river basin covers a drainage area of 205 km^2 with an average gradient of 52.2% and elevations ranging within 900–1100 m (Fang et al., 2007a, b). The drainage basin is predominated by a semiarid landscape with nearly constant vegetation coverage. The grass and forest coverages are about 10% and 10%–15%, respectively (Wang 1991). The sparse vegetation on this region is mainly caused by a temperate continental monsoon climate characterized by widespread drought and low precipitation. The annual precipitation in the basin presents an average of 480 mm with significant intra- and inter-annual variability from 1959 to 1969; moreover, about 70% of the precipitation is mainly concentrated between June and September (Cai et al. 2004). The rainstorms in this area typically have short duration and high intensity (up to 3.5 $mm \cdot min^{-1}$). The annual runoff depth from the basin has an average of 54 mm between 1959 and 1969, and >62% of the runoff occurs throughout the months from June to September. The average annual water surface evaporation reaches as high as 1570.4 mm between 1954 and 1958, and the annual average temperature is 8 °C, ranging from −27 °C to 38 °C. About 183 frost days are present each year. The soil type of the original landscape belongs to sandy loess, which exhibits a fine-loamy texture with 46.1%, 48.7%, and 5.2% of sand, silt, and clay contents, respectively (Liu et al. 2000). Soil erosion in this region is severe because of extremely high rainfall intensity and high susceptibility of the soil to rainfall-runoff detachment. The annual sediment yield varies from 0.63×10^4 t km^{-2} to 2.37×10^4 t km^{-2} between 1954 and 1958, with an average yield of 1.58×10^4 t km^{-2}. In the current study, Tuanshangou (a sublateral of Shejiagou), Shejiagou (a first branch of Chabagou), and the Chabagou trunk were selected to examine the spatial scale effect on event-based sediment dynamics in basin-wide floods in the basin system. The location of the study sites is shown in Fig. 1, and the characteristics of the study gullies/channels are listed in Table 1.

2.2. Data sources and treatments

The runoff experimental station was managed by the Yellow River Conservancy Commission (YRCC) of the Ministry of Water Resources of People's Republic of China (PRC) between 1959 and 1969. The Tuanshangou Sloping Runoff Field, 60 rain gauges, and 9 hydrometric gauging stations were established in the Chabagou basin (Fig. 1) to collect flow and sediment data for the soil erosion and sediment yield research. All the measurements of water stage, water discharge, total runoff, suspended sediment concentration and grain size, and sediment load followed the national standards issued by the YRCC (1959 to 1969). The procedures used for hydrological survey, sampling, and laboratory analyses at hydrometric stations are basically in accordance with international standards (Xu 1999). For a more detailed information, kindly refer to Zheng et al. (2011); Zheng et al. (2012), and Zheng et al. (2015). All the data of water discharge and suspended sediment load were obtained from the YRCC (1961–1971). The flow and sediment data utilized in the current study involved three spatial scales (sublateral, branch, and trunk) in the Chabagou basin system (Table 1).

To investigate the spatial behavior of sediment flow by a single rainstorm flood event, individual basin-wide flood events should be segregated from all the recorded events. Single complete flow lines and sediment routes induced by basin-wide flood events should be included in these individual events in terms of consistence and continuity of tempo-spatial scales. These flow lines and sediment routes should start from the Tuanshangou sub-basin, passing by the Shejiagou branch, emptying into the Chabagou trunk, and should terminate at the basin outlet (the Caoping station). The beginning of the rising limb and the time-to-peak (T_p) of each flood hydrograph were determined using the antecedent water discharge with low suspended sediment concentration and occurrence of the flood peak discharge. The travel duration (D_t) of the flood crest across the studied scale levels for each flood hydrograph was also calculated. At-a-station velocity–discharge relations were regressed using the recorded measurements of flow velocity and discharge with the widely used hydraulic geometry relations in terms of power function model (Ferguson 1986; Leopold and Maddock 1953; Singh and Zhang 2008). The flow velocity at the Shejiagou station can be described by the following power function equation of water discharge with R^2 ranging within 0.74–0.98. In addition, the number of effective samples for the studied events each year varies from 14 to 86 between 1961 and 1969.

$$V_i = kq_i^m \tag{1}$$

where V_i ($m \cdot s^{-1}$) is the mean flow velocity; q_i ($m^3 \cdot s^{-1}$) is at-a-station instantaneous water discharge; coefficient k is a scale factor, which varies from 0.67 to 1.65; and parameter m is an exponent, which varies from 0.31 to 0.52. Velocity measurements were not conducted at the Tuanshangou station. Thus, the velocity–discharge relations derived from the Shejiagou station were also applied at the Tuanshangou station because of the short distance between these two stations.

Therefore, for any stream of upstream water discharge at one smaller scale, the travel time it takes to reach the gully/channel of the next level at a larger scale can be estimated by dividing the channel length by the mean flow velocity, assuming that the channel length is L:

$$D_i = \frac{L}{V_i} \tag{2}$$

where D_i (min) is the travel duration for any stream of water discharge flowing from the upstream station to the downstream station, and L (m) is the channel length.

D_t has already been calculated from the flood hydrograph, which also matches Eqs. (1) and (2):

$$D_t = \frac{L}{kq_p^m} \tag{3}$$

where D_t (min) is the travel duration for flood crest flowing from the upstream station to the downstream station; q_p ($m^3 \cdot s^{-1}$) is the flood peak discharge.

Subsequently, D_i can be obtained with a combination of Eqs. (1)–(3)

$$D_i = D_t \cdot \left(\frac{q_p}{q_i}\right)^m \tag{4}$$

On the basis of the event-based flood hydrographs and numerous trials and errors from Eq. (4), the temporal scales, that is, the beginning and terminating time of single flow lines and sediment routes at different spatial scale levels, were empirically and reasonably determined. A total of 44 basin-wide flood events consisting of 44 single-flow lines and sediment routes from the upstream Tuanshangou sub-basin to the downstream Chabagou trunk (the Caoping station) were determined. Therefore, further analyses regarding spatial scale dependency of flow and sediment processes were conducted under near-natural condition with little human disturbance. In addition, event runoff amount (Q), sediment load, and sediment yield (ESY) were calculated, depending on the recorded measurements of water discharge, time interval, and suspended sediment concentration. Event runoff amount and flood peak discharge (q_p) were normalized to the drainage area, and thus event runoff depth (H) and flood peak discharge modulus (D_p) were obtained. The event-based average suspended sediment concentration (SCE) was obtained by dividing the event sediment yield by the event runoff amount. Similarly, the area-specific sediment yield (SSY) was computed by normalizing the event sediment yield to the basin drainage area. Statistical analyses were conducted with SPSS 18.0, through which equations were generated. All the graphics were plotted using SigmaPlot 12.0 software.

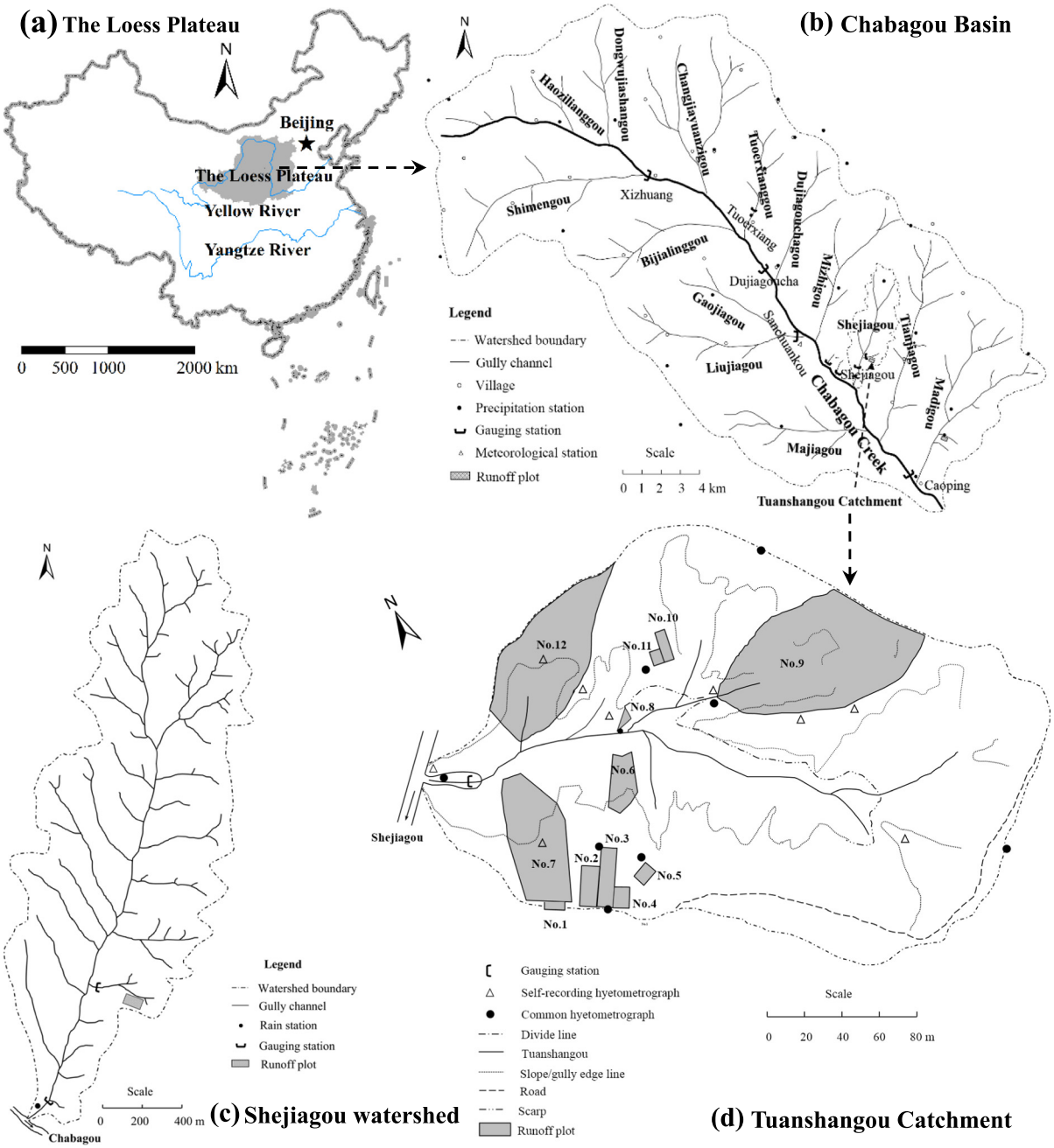

Fig. 1. Location of the study area in Chabagou River basin.

Table 1
Characteristics of gullies/channels in the Chabagou basin system[a].

Gully/channel at different scale levels	Gauging station	Drainage area (km^2)	Average gully channel gradient (‰)	Drainage density ($km\ km^{-2}$)	Drainage type	Annual average runoff depth (mm)	Sediment delivery ratio	Number of recorded events	Period of data available
Tuanshangou	Tuanshangou	0.18	135	0.63	Sublateral		1	93	1961–69
Shejiagou	Shejiagou	4.26	11.5	0.78	Branch	55.6	0.83	49	1960–69
Chabagou	Caoping	187	7.57	1.05	Trunk	56.8	1.1	64	1959–69

[a] Drainage density after Mu and Meng (1982) and Fang et al. (2008); Annual average runoff depth and sediment delivery ratio after Chen (2001).

3. Results

3.1. Characteristics of event-based water flows and sediment delivery across scales

The spatial scale behavior of event-based water flows and sediment delivery is presented in Table 2. High scale-specific inter-event variability is evident across scales from the Tuanshangou sub-basin to the Chabagou trunk (the Caoping station). In terms of flow-related variables, T and T_p experience a climbing trend. However, H and D_p show a declining trend as the drainage area increases. This result indicates the combined effects of rainfall types and the heterogeneity of topographic-hydrological conditions underlying the basin surface on the spatial behavior of event-based runoff generation and routing schemes. Coefficients of variance of flow-related variables are mostly larger than 1, hence revealing the high inter-event variability within a single scale. In terms of event-based sediment delivery, *SSY* undergoes incipient decrease, followed by a subsequent increase with the increase in drainage area. This result indicates that the sediment flow behavior is mainly controlled by the depositional process from the Tuanshangou sublateral to the Shejiagou branch. On the contrary, the sediment flow is associated with erosional process from the Shejiagou branch to the Chabagou trunk. Deduced from the coefficients of variance of *SSY* (larger than 1), the scale-specific sediment process is also subject to high inter-event variability. However, both *SCE* and *MSCE* show relatively low variability with much smaller coefficients of variance. Specifically, *SCE* increases with the increase in drainage area, and *MSCE* first declines slightly at the Shejiagou station and subsequently rises at the basin outlet. Such observation implies the variation in sediment transport capacity of hyperconcentrated flow along the distance. Additionally, the coefficients of variance of almost all the examined variables exhibit a general dropping tendency from the Tuanshangou station to the Caoping station. This tendency indicates that the inter-event variability diminishes, and the sediment flow behavior tends to be increasingly steady with the increase in drainage area.

One-way ANOVA was conducted via Tukey's test for multiple comparisons to compare the examined event-based variables between studied scale levels (Table 2). Overall, no significant difference was observed for T_p, H, and *SSY* between Tuanshangou, Shejiagou and Caoping stations. This result indicates the spatial invariability of the *SSY-H* relationships. The spatial independency of *SSY-H* relationship was validated at length in previous studies conducted by Zheng et al. (2012, 2013). The invariant relationship also accords with the general common phenomenon that more water flow can produce more sediment, despite the change of spatial scale. However, T, D_p, *SCE*, and *MSCE* at the Tuanshangou and Shejiagou stations are significantly different from those at the Caoping station, and little discrepancy exists between the Tuanshangou and Shejiagou stations. Such difference implies that T, D_p, *SCE*, and *MSCE* are dependent on spatial scale, particularly from the Shejiagou branch to the Chabagou trunk. ANOVAs were also conducted to test the discrepancy for Q, *ESY*, and q_p among the examined scale levels. The Q and *ESY* at the Caoping station are significantly larger than those at the Tuanshangou and Shejiagou stations. Nevertheless, little difference was observed between the Tuanshangou and Shejiagou stations. q_p also exhibits a climbing trend with significant discrepancy across all the scale levels. The spatial dependency of Q, *ESY*, and q_p is to some extent offset when normalized to the drainage area. The difference may be attributed to the presence of nonlinear relations among sediment yield, runoff yield, and environmental factors (Parsons et al. 2004, 2006; Roering et al. 1999; Vente et al. 2011; Wilcox et al. 2003). As a typical soil erosion response, suspended sediment concentration reflects the proportion relationship of the amount of sediment carried by the flowing water to the total amount of the water–sediment mixture. Thus, minimal influence by the spatial dependency of runoff yielding is exerted on the suspended sediment concentration across sites. Consequently, suspended sediment concentration is more suitably used to explore the spatial behavior of the process of soil erosion and sediment delivery, which is similar to the investigations conducted by Fang et al. (2008); Zheng et al. (2011); Zheng et al. (2013), and Zheng et al. (2015).

Table 2
Descriptive statistics of event-based flow and sediment across studied scales.

Variables	Scale level	Statistical description				N
		Min	Max	Mean[*]	CV	
T/min	Tuanshangou	35	1092	168[b]	1.12	44
	Shejiagou	64	1425	271[b]	0.89	44
	Chabagou	138	1645	441[a]	0.56	44
T_p/min	Tuanshangou	3	314	47[a]	1.56	44
	Shejiagou	3	465	55[a]	1.94	42
	Chabagou	2	312	60[a]	1.31	40
D_p/$m^3 \cdot km^{-2} \cdot s^{-1}$	Tuanshangou	0.0028	70.56	10.1[a]	1.67	44
	Shejiagou	0.0065	22.3	3.59[a]	1.53	44
	Chabagou	0.0049	8.13	1.18[b]	1.38	44
H/mm	Tuanshangou	0.01	31.6	5.6[a]	1.46	44
	Shejiagou	0.03	30.3	5[a]	1.37	44
	Chabagou	0.1	35.6	4.7[a]	1.32	44
SSY/$t \cdot km^{-2}$	Tuanshangou	0.03	23,710	3912[a]	1.6	44
	Shejiagou	0.08	19,240	3285[a]	1.48	44
	Chabagou	7.46	27,859	3522[a]	1.41	44
SCE/$kg \cdot m^{-3}$	Tuanshangou	5.67	887	497[b]	0.49	44
	Shejiagou	1.73	829	524[b]	0.45	44
	Chabagou	69.5	997	679[a]	0.28	44
$MSCE$/$kg \cdot m^{-3}$	Tuanshangou	11.9	1030	639[b]	0.42	44
	Shejiagou	1.9	953	634[b]	0.41	44
	Chabagou	83	1220	800[a]	0.24	44

CV, Coefficient of variance; *N*, the number of selected events in statistical analysis; T, duration of the individual flood hydrograph at different spatial scales; T_p, time-to-peak, that is, the time from the beginning of the rising limb to the occurrence of the flood peak discharge; D_p, flood peak discharge modulus; H, event runoff depth; *SSY*, event area-specific sediment yield; *SCE*, event-based average suspended sediment concentration; *MSCE*, event-based maximum suspended sediment concentration.[*], means for each variable determined with different letter designations are significantly different across studied scale levels ($P \leq 0.05$).

3.2. Intra- and inter-scale flow–sediment relationships

As a basic erosive agent, rainfall-triggered surface runoff is the main driving force inducing soil detachment and resultant sediment export at the basin outlet. Several runoff-related factors and derived variables or combined parameters, such as total/unit discharge, runoff depth, flow shear stress, total stream power, and runoff-energy factor were previously proposed to describe site-specific flow–sediment relationship (Williams and Berndt 1977; Bonta 2000; Knapen et al. 2007). However, the feasibility of these indicators in explaining the event-based scale interactions of sediment-laden flow across sites has not yet been extensively analyzed. Therefore, several indicators were selected to conduct the examination. The selected indicators, apart from those conventionally used in Section 3.1, are given as follows.

The runoff-energy factor (*RE*) is calculated by Williams and Berndt (1977) as follows:

$$RE = Q \cdot q_p \tag{5}$$

where Q (m^3) is the total runoff volume, and q_p ($m^3 \cdot s^{-1}$) is the flood peak discharge.

The unit runoff-energy factor (RE_u, $m^4 \cdot s^{-1}$) is defined as the *RE* factor per unit area and obtained by normalizing the *RE* factor to the basin drainage area

$$RE_u = q_p \cdot H \tag{6}$$

Flow shear stress (τ, $N \cdot m^{-2}$) is calculated using the following equation (Xu 1999, 2004):

$$\tau = \gamma_m gHJ \tag{7}$$

where g ($m \cdot s^{-2}$) is the acceleration caused by gravity (9.8); H (m) is the runoff depth; and J is the average gradient, and γ_m is given as follows:

$$\gamma_m = S + \gamma \cdot (1 - S/\gamma_s) \tag{8}$$

where γ_m ($kg \cdot m^{-3}$) is the mass density of water–sediment mixture; S ($kg \cdot m^{-3}$) is the average suspended sediment concentration; γ ($kg \cdot m^{-3}$) is the mass density of pure water; and γ_s ($kg \cdot m^{-3}$) is the sediment density, which is generally 2650.

Stream power (ω, $W \cdot m^{-1}$), which is modified from Xu (1999) and Knighton (1999), is calculated by the following equation:

$$\omega = \gamma_m g q_p J \tag{9}$$

The stream energy factor, which is termed SE (W), is proposed by introducing H into Eq. (9) and calculated as follows:

$$SE = \gamma_m g q_p HJ \tag{10}$$

Regression analysis was performed to establish the intra-scale flow–sediment relationship by linking SCE, $MSCE$, and ESY to the abovementioned flow-related indicators. The results are presented in Table 3.

All the regression results are statistically significant with $sig \leq 0.001$; —, the results for equations with $R^2 < 0.5$ are not given in the table, which is the same below.

A general increasing trend toward higher SCE and $MSCE$ and larger ESY associated with greater q_p and Q is clearly evident in Table 3. SCE and $MSCE$ show significantly linear correlation with the logarithm of ω, SE, RE_u, q_p, and H. In addition, they increase as a positive exponential function of flow shear stress with negative exponents. The regression equation for each runoff-based indicator also indicates the existence of detachment-limited maximum suspended sediment concentration for a region with nearly unlimited sediment supply (Fig. 2). Generally, SCE and $MSCE$ increase rapidly to the maximum at a low level of each indicator examined and subsequently remain relatively constant. The sediment rating curves imply that hyperconcentrated flow-driven erosion is a detachment-limited process across sites, despite the operation of positive feedback effects entailing the further increase in sediment concentration (Xu 1999, 2004). Accordingly, the event-extreme suspended sediment concentration can be regarded as the detachment-limited maximum sediment-carrying capacity (Zheng et al. 2012). ESY acts as a simple linear function of Q or SE to increase, and it can also be well described as power functions of RE, q_p, and ω.

To further examine the inter-scale flow–sediment relationship, variables indicative of inter-scale variations in Q, q_p, τ,ω, RE, SE, and RE_u were used to fit the variables indicative of inter-scale variations in SCE, $MSCE$, and ESY. Considering the validity of the parameters and the detainment of scale-specific information, the selected variables and calculation methods are given as follows:

$$\Delta X = X_j - X_i \qquad \Delta Y = Y_j - Y_i \tag{11}$$

$$X_R = X_j / X_i \qquad Y_R = Y_j / Y_i \tag{12}$$

where X represents the measured value of each sediment-relevant variable, including SCE, $MSCE$, and ESY; Y represents the measured or calculated value of each runoff-related indicator, including Q, H, q_p, RE, RE_u, τ, ω, and SE; Δ represents the actual inter-scale difference of each selected variable across sites; X_R and Y_R represent the inter-scale ratio of each corresponding variable across any two sites; i and j represent the different scale levels with $i = 1, 2$ and $j = 2, 3$, whereas $i \neq j$; 1, 2, 3 represent the Tuanshangou (sublateral), Shejiagou (branch), and Caoping (Chabagou trunk) stations, respectively.

Regression analyses with significance test were performed between ΔX, X_R and ΔY, Y_R. Moreover, ΔXs, X_Rs were plotted against ΔYs, Y_Rs (Fig.3). Hence, the regression equations were obtained (Table 4).

In terms of inter-scale difference of suspended sediment concentration, ΔSCE and $\Delta MSCE$ increase with the logarithmic–linear equations of inter-scale ratio of main flow-related indicators. Individually, the inter-scale ratio of stream energy demonstrates the most satisfactory performance, whereas that of flow shear stress performs the least (Fig. 3a and c). This result indicates that variations of suspended sediment concentration in the basin system can be better described with energy-related variables than mechanics-related variables. Furthermore, the critical inter-scale ratio of flow-related variables rendering the same SCE or $MSCE$ in downstream flow as that in upstream flow, that is, ΔSCE or $\Delta MSCE$ is 0, can be obtained using the regression equations in Table 4.

Thus, if $\Delta SCE = 0$, we obtain the following:

$SE_R = 1.2$, $\omega_R = 1.7$, $RE_{uR} = 6.9$, $H_R = 0.6$, $q_{pR} = 2.9$, $\tau_R = 0.2$.

If $\Delta MSCE = 0$, we obtain the following:

$SE_R = 1.7$, $\omega_R = 2.2$, $RE_{uR} = 10$, $H_R = 0.7$, $q_{pR} = 12.6$, $\tau_R = 0.08$.

The critical values of the inter-scale ratio imply that the sustainability of the same SCE requires 0.2, 0.7, 5.9, and 1.9-time increase in SE, ω, RE_u, and q_p in the downstream direction across sites, respectively. A similar trend exists in the variations of the $MSCE$ with the abovementioned flow-related variables. Conversely, the sustainability of the same SCE and $MSCE$ in both upstream flow and downstream flows does not require an increase in τ to maintain the suspended load motion and sediment transport equilibrium (Xu 1999). Such observation can be explained by the decreased energy expenditure on the suspended load motion caused by the decrease in flow resistance with the increase in suspended sediment concentration, as indicated by Shu et al. (2008) with lab flume experiments for hyperconcentrated flows.

With respect to the inter-scale difference and ratio of sediment yield, ΔESY linearly increases with the increase in ΔSE and ΔQ. Otherwise, ΔESY can be described with power equations of ΔRE and Δq_p. Additionally, ESY_R is positively and linearly correlated with SE_R, ω_R, RE_R, Q_R, and q_{pR}, (Table 4). Overall, Δq_p and q_{pR} perform the best to fit ΔESY and ESY_R (Fig. 3e and f). The increase in ESY induced by per unit increase in q_p or Q across studied scales is therefore obtained. On the average,

Table 3
Regression results of event-based flow–sediment relationship in the basin system.

Indicators	$SCE/kg \cdot m^{-3}$		$MSCE/kg \cdot m^{-3}$		ESY/kg		N
	Equation	R^2	Equation	R^2	Equation	R^2	
Q/m^3	–	–	–	–	$ESY = 784.01Q$	0.99	132
$q_p/m^3 \cdot s^{-1}$	$SCE = 61.1\ln q_p + 461$	0.58	$MSCE = 61.2\ln q_p + 585.2$	0.51	$ESY = 4.42 \times 10^5 q_p^{1.36}$	0.96	132
H/mm	$SCE = 110.6\ln H + 489.3$	0.56	$MSCE = 118.5\ln H + 607.9$	0.57	–	–	132
$\tau/N \cdot m^{-2}$	$SCE = e^{6.35} e^{-0.023/\tau}$	0.61	$MSCE = e^{6.58} e^{-0.022/\tau}$	0.67	–	–	132
$\omega/W \cdot m^{-1}$	$SCE = 87.7\ln\omega - 85.2$	0.76	$MSCE = 90.4\ln\omega + 18.6$	0.72	$ESY = 436.28\omega^{1.68}$	0.84	132
$RE/m^6 \cdot s^{-1}$	–	–	–	–	$ESY = 4101RE^{0.64}$	0.97	132
$RE_u/m^4 \cdot s^{-1}$	$SCE = 46.2\ln RE_u + 773.5$	0.67	$MSCE = 47.3\ln RE_u + 902.7$	0.63	–	–	132
SE/W	$SCE = 53.3\ln SE + 501.4$	0.73	$MSCE = 55.8\ln SE + 622.5$	0.71	$ESY = 10^7 SE$	0.86	132

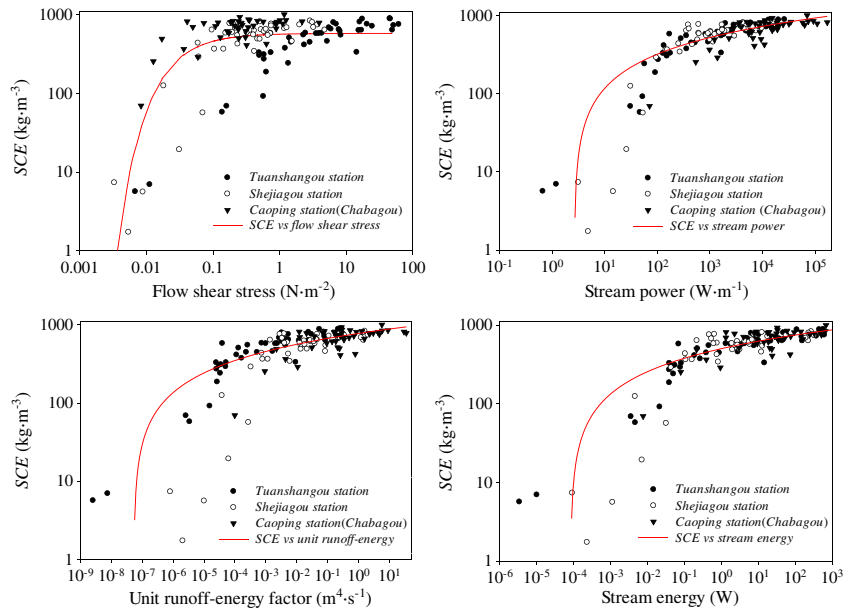

Fig. 2. Event-based flow–sediment relationships in the basin system. The results obtained from regression analysis of *SCE* are similar to those from *MSCE*, which are not given in the figure.

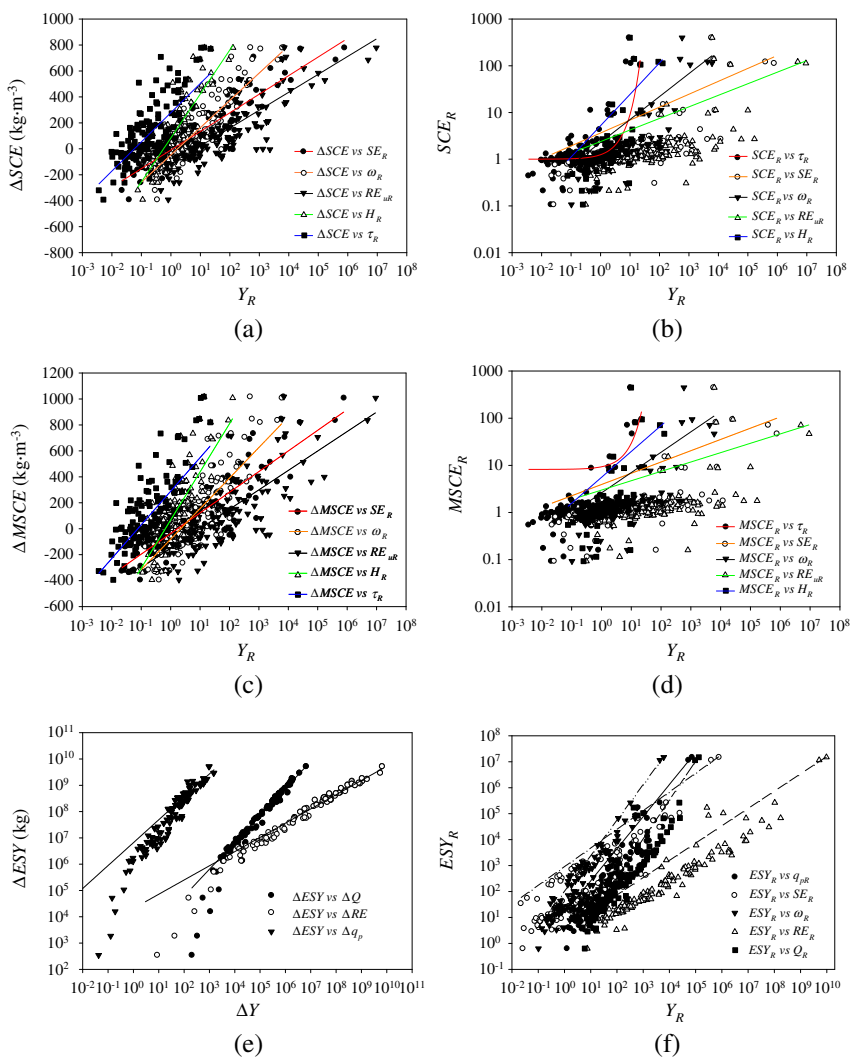

Fig. 3. Relationships of ΔX, X_R to ΔY, Y_R.

Table 4
Regression results of event-based inter-scale flow-sediment relationship.

Indicators	ΔSCE/kg·m^{-3}		$\Delta MSCE$/kg·m^{-3}		ΔESY/kg		ESY_R	
	Fitted equations	R^2	Fitted equations	R^2	Fitted equations	R^2	Fitted equations	R^2
$SE_R/\Delta SE$	$\Delta SCE = 62.3\ln SE_R - 9$	0.76	$\Delta MSCE = 69.1\ln SE_R - 36.9$	0.70	$\Delta ESY = 1\times10^6\Delta SE + 3\times10^8$	0.82	$ESY_R = 21.4SE_R$	0.96
ω_R	$\Delta SCE = 91.5\ln\omega_R - 47.1$	0.71	$\Delta MSCE = 102.3\ln\omega_R - 80.7$	0.65	–	–	$ESY_R = 2445.9\omega_R$	0.96
$RE_{uR}/RE_R/\Delta RE$	$\Delta SCE = 60\ln RE_{uR} - 115.9$	0.69	$\Delta MSCE = 65.1\ln RE_{uR} - 1497$	0.60	$\Delta ESY = 2726.2\Delta RE^{0.66}$	0.96	$ESY_R = 0.0017RE_R$	0.97
$H_R/Q_R/\Delta Q$	$\Delta SCE = 147.3\ln H_R + 84.3$	0.67	$\Delta MSCE = 161.2\ln H_R + 67.3$	0.59	$\Delta ESY = 785.5\Delta Q$	0.99	$ESY_R = 109.3Q_R$	0.94
$q_{pR}/\Delta q_p$	$\Delta SCE = 185.4\ln q_{pR} - 195$	0.60	$\Delta MSCE = 92.1\ln q_{pR}$-233.6	0.51	$\Delta ESY = 7\times10^5\Delta q_p^{1.29}$	0.99	$ESY_R = 206.5q_{pR}$	0.99
τ_R	$\Delta SCE = 197.9\ln\tau_R + 279.1$	0.52	$\Delta MSCE = 112.6\ln\tau_R + 289.2$	0.51	–	–	–	–

ESY increases by approximately 0.8 t when *Q* increases by 1 m^3 in the downstream direction. Comparatively, about 700 t increase in *ESY* is caused by 1 m$^3\cdot$s^{-1} increment in q_p in the downstream direction, and the increase rate increases as a power function of the increment in q_p ($9\times10^5\Delta q_p^{0.29}$). This result implies that *ESY* across scales is more largely driven by q_p than *Q*. Therefore, variations of sediment-relevant variables seems to be more susceptible to flow-related variables incorporating q_p.

3.3. Event-based contribution of upstream sediment-laden flow to downstream sediment delivery

In terms of event-based Shejiagou–Tuanshangou relationships at sublateral-branch scale, *SCE* and *MSCE* at the Shejiagou station show a general climbing trend as a power function of *SCE* at the Tuanshangou station (Eq. (13), Fig. 4a). However, correlations of inter-scale relationships for *SCE* and *MSCE* decrease drastically when the scale of the study scope enlarges to branch-trunk level (Eq. (14), Fig. 4b). Clearly, the effect of upstream sediment flows on suspended sediment concentration in downstream flows becomes limited from sublateral-branch scale to branch-trunk scale. Thus, the spatial dependency of event-based suspended sediment concentration decreases with the increment in basin drainage area. Nevertheless, if minor sediment-producing events with $SSY < 300$ t·km^{-2} were excluded, the coefficient of determination decreases to some extent at sublateral-branch and branch-trunk scales (Eqs. (15) and (16)). Hence, less impact by hyperconcentrated flows than low-concentration flow upstream is exerted on the suspended sediment concentration dynamics in hyperconcentrated flows downstream.

$$\begin{cases} SCE_{she} = 0.19SCE_{tuan}{}^{1.24}, N = 44, R^2 = 0.76, P<0.001 \\ MSCE_{she} = 0.48MSCE_{tuan}{}^{1.12}, N = 44, R^2 = 0.73, P<0.001 \end{cases} \quad (13)$$

$$\begin{cases} SCE_{cha} = 0.35SCE_{she} + 493, N = 44, R^2 = 0.19, P = 0.003 \\ MSCE_{cha} = 545.5e^{0.001MSCE_{she}}, N = 44, R^2 = 0.11, P = 0.028 \end{cases} \quad (14)$$

$$\begin{cases} SCE_{she} = 0.64SCE_{tuan} + 215.6, N = 27, R^2 = 0.59, P<0.001 \\ MSCE_{she} = e^{7.14}e^{\frac{-410.3}{MSCE_{tuan}}}, N = 27, R^2 = 0.45, P<0.001 \end{cases} \quad (15)$$

$$\begin{cases} SCE_{cha} = 17.7SCE_{she}{}^{0.58}, N = 32, R^2 = 0.37, P<0.001 \\ MSCE_{cha} = 111.8MSCE_{she}{}^{0.30}, N = 32, R^2 = 0.08, P = 0.12 \end{cases} \quad (16)$$

where SCE_{tuan}, SCE_{she}, and SCE_{cha} are *SCEs* at the Tuanshangou, Shejiagou, and Caoping stations, respectively; correspondingly, $MSCE_{tuan}$, $MSCE_{she}$, and $MSCE_{cha}$ are their *MSCEs*.

Correlation and regression analyses were performed to ascertain the quantitative influence of suspended sediment concentration in upstream flows on downstream sediment yield. *ESY* at the Shejiagou station is closest to the *SCE* at the Tuanshangou station with a positive

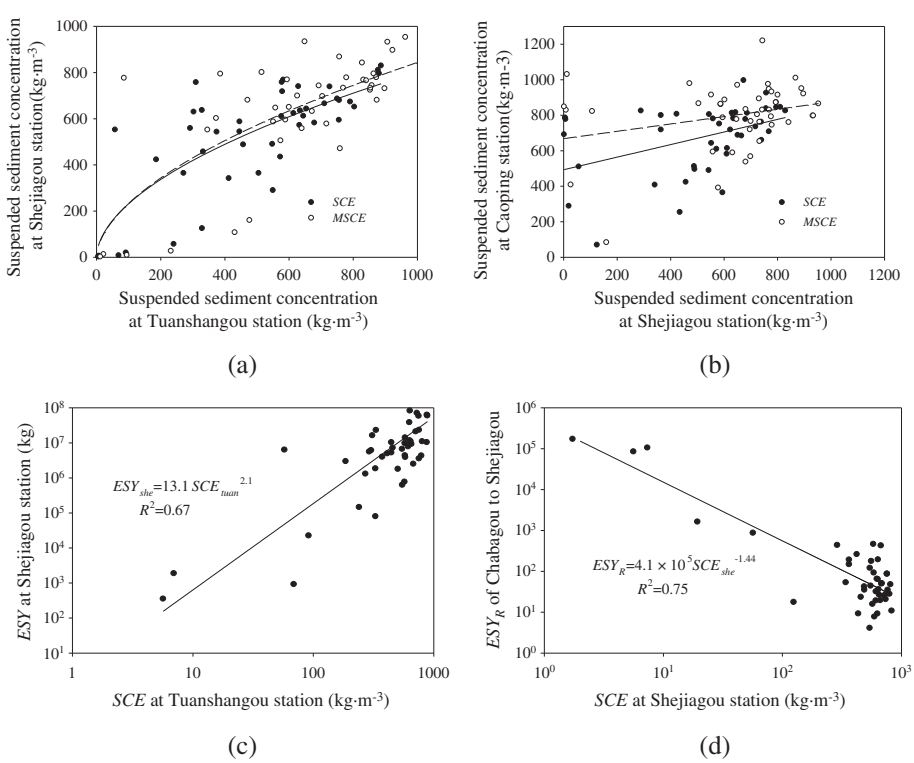

Fig. 4. Effect of suspended sediment concentration in upstream flow on sediment delivery in downstream flow across scales.

power function relationship ($P < 0.001$, Fig. 4c). The inter-scale ratio of *ESY* shows a significantly decreasing trend as a negative power equation of *SCE* at the Shejiagou station ($P < 0.001$, Fig. 4d). Therefore, the sediment-laden flow upstream is an important promoting contributor for downstream sediment export at sublateral-branch scale. However, the increase in suspended sediment concentration in upstream flow alleviates the further increase in the sediment load of flowing water downstream. Nevertheless, for major sediment-producing events with $SSY \geq 300\ t \cdot km^{-2}$, the inter-scale ratio of *ESY* at sublateral-branch and branch-trunk scales exhibits an exponential and power relationship with *SCE* at the Tuanshangou and Shejiagou stations. The decreased R^2 of the regression equations (Eqs. 17 and 18) also indicates that the spatial scale effect on *ESY* diminishes with the increase in basin drainage area, specifically for hyperconcentrated flows.

$$ESY'_R = 181.5e^{-0.003SCE_{tuan}}, N = 27, R^2 = 0.52, P<0.001 \quad (17)$$

$$ESY_R = 1.5 \times 10^5 SCE_{she}{}^{-1.24}, N = 32, R^2 = 0.08, P = 0.11 \quad (18)$$

where ESY_R' and ESY_R are the inter-scale ratios of *ESY* at sublateral-branch and branch-trunk scales, respectively.

4. Discussion

4.1. Spatial independency of event-based suspended sediment concentration in the basin system

The event-based suspended sediment concentration increases with the enlargement of spatial scale, and the variance coefficient also decreases in the downstream direction in the basin system (Table 2). Studies on major sediment-producing events conducted by Zheng et al. (2011) and Zheng et al. (2012) also showed similar results at the sub-watershed and watershed scales. This result indicates the proneness of suspended sediment concentration to be scale-specific steady with the increase in drainage basin area. As illustrated in Fig. 3b, and d, a large number of scatters fall around the ratio of 1, thereby manifesting the spatial invariability of suspended sediment concentration, specifically in hyperconcentrated flows. According to Zheng et al. (2013) and Zheng et al. (2015), as a result of a sufficient sediment supply provided by the active mass wastings, suspended sediment concentration in most water flows can reach the detachment-limited maximum when departing from sloping surfaces and entering the headwater basin of the first-order channels (sub-watershed). Subsequently, this concentration remains spatio-temporally invariant in the basin system. The power function relationship developed between event mean sediment concentration and drainage basin area by Zheng et al. (2011) also indicated the spatial invariability of sediment concentration in hyperconcentrated flows.

The event-based relationship between suspended sediment concentration and flow-related indicators can be described by logarithmic–linear functions, except for τ (Table 3). The event-based relationships between $\Delta MSCE$, ΔSCE and inter-scale difference of main flow-related indicators (ΔYs) can also be effectively simulated with logarithmic–linear equations across studied scale levels (Table 4, Figs. 3a, and 3c). Furthermore, the consistency in function structure signifies the uniformity of flow–sediment concentration relationship in the basin system. The spatio-temporal invariability of flow-sediment relationship in hyperconcentrated flows was also previously reported by Zheng et al. (2013). Additionally, the spatial independency of flow–sediment concentration relationship can be further confirmed by an event-based inter-scale relationship depicted in Figs. 3b and d. This relationship can be regressed as power function equations (not given in Table 4). The results shown in Tables 3 and 4 and Fig. 4 indicate that the mechanism underlying the sediment delivery does not vary in the downstream direction in the basin system.

4.2. Mechanism of event-based sediment delivery driven by hyperconcentrated flows

Soil erosion caused by concentrated flow is highly dependent on flow conditions. An effective approach in estimating spatial and temporal soil losses is to link erosion rates to simple hydraulic parameters or composite predictor variables derived from them (Knapen et al., 2007). Generally, these parameters or predictor variables can be classified into two categories, namely, mechanics- and energy-related variables, as examined in Tables 3 and 4. The fitting results show that energy-related variables (ω and *SE*) perform better in describing event-based intra- and inter-scale flow–sediment relationships than mechanics-related variables (τ).

The runoff depth is directly related to the surface runoff; thus, the former is widely used to estimate the sediment production at watershed outlet alone. However, the developed model may be more appropriate in predicting the sediment yield from major sediment-producing events (Zheng et al. 2011, Zheng et al. 2012, Zheng et al. 2013). For minor sediment-producing events, final sediment export may be dramatically underestimated by those models. Water flow, which is associated with the soil erosion it induces, is a process-specific concept. Nevertheless, runoff depth, a proxy for runoff volume, cannot account for the complete information on the process of runoff yield and concentration. Thus, the amount of surface runoff only indicates the potential capability of water flows to detach soil particles and deliver sediments instead of determining the ultimate sediment output. Consequently, sediment yield may be substantially misestimated for major runoff events with minor peak discharge and minor runoff events with major peak discharge. Table 4 shows that flood peak discharge is more suitable than runoff amount in predicting inter-scale difference and ratio of sediment yield across studied scales. On the average, the increment in sediment yield caused by per 1 $m^3 \cdot s^{-1}$ increase in flood peak discharge is at least 875 times of that caused by per 1 m^3 increase in runoff amount in the downstream direction. Cai et al. (2004) also suggests that the effect of runoff depth on sediment yield slightly varies across sites at the watershed scale, and runoff variability is an important driving factor to cause significant difference in sediment output across different spatial scales. In addition, the proposed stream energy factor, which incorporates flood peak discharge and event runoff depth, shows some advantages in simulating the event-based inter-scale flow–sediment relationship over other predictor variables. These results indicate that integrating process-based variables into predictors for sediment yield estimation will highlight the process-specific conception of soil erosion, although the estimation results may not be largely improved (Zheng et al. 2015).

4.3. Implications for sediment control and benefit evaluation of sediment control strategies

Sediment control should be process-oriented and aimed at altering the original inter-scale flow–sediment relationship by reducing the runoff erosivity and precluding the occurrence of hyperconcentrated flows in the basin system. As an important gully erosion control measure, check dam plays an indispensable role in base-level uplift and grade elimination (Xu 1999). Both flood runoff volume and flood peak discharge will be severed, that is, the flood runoff pattern will be changed because of the construction of check dams. Thereby, the runoff erosivity will be reduced, and the connectivity of hyperconcentrated flows will be cut off. Accordingly, the decrease of sediment-carrying capacity of water flows will be achieved. As a result, the effect of different flood runoff patterns on the process of sediment yielding also needs further investigation under different situations to fill the gaps and overcome the limitations. Several studies on the vegetation effects on runoff–sediment yield relationship were carried out at different spatial scales, which enriched the related knowledge on the function of vegetation in soil and water conservation (Zheng et al., 2007a, b). Consequently,

efficiency assessment of sediment control measures should be based on the process of runoff regulation. Both explicit sediment reduction by decreasing runoff volume and implicit sediment reduction by altering flow–sediment relationship should be determined further. This enables a more rational-based benefit evaluation toward a comprehensive efficiency assessment of soil erosion control strategies in reducing sediment export.

5. Conclusion

Data of sediment and run-off yield on 44 basin-wide flood events were collected in this study. Thus, analyses on the spatial scale dependency of sediment dynamics were performed throughout the studied basin system.

In the basin system, event-based suspended sediment concentration and intra- and inter-scale flow–sediment relationships remain spatially invariant. Therefore, the multitude of sediment-laden flows can reach at detachment-limited maximum sediment carrying capacity across different spatial scales. As a result, the influence of upstream sediment-laden flow on downstream sediment output is also limited, particularly for major sediment-producing events.

The inter-scale flow–sediment relationships are well described by logarithmic–linear functions. The inter-scale difference in event sediment yield is better interpreted by variations in flood peak discharge than by those in runoff amount. To embody the process-specific characteristics of soil erosion, parameters indicative of runoff amount and flow strength should be incorporated into the predictor variables for sediment yield estimation.

Event flood runoff volume, peak discharge, and flood duration will be changed (decreased, cut down, and prolonged, respectively) because of the detention storage capacity of check dams; that is, the flood runoff pattern will be altered if check dams are widely implemented on gullies. To date, significant attention has been given to the explicit or direct sediment reduction benefits indicated by on-site trapped sediments. However, the implicit or indirect sediment reduction benefits underlying the conversion between different flood runoff patterns have not yet been intensively quantified. Thus, the influence of altered flood runoff pattern on flow–sediment relationship and sediment export needs a further investigation. Consequently, overall assessments might be established on sediment control benefits caused by anti-erosion strategies.

Acknowledgements

This research was financially supported by the National Natural Science Foundation of China (Grant No. 41330858). We also appreciate the suggestions of an anonymous reviewer and editor.

References

Bagarello, V., Ferro, V., Giordano, G., 2010. Testing alternative erosivity indices to predict event soil loss from bare plots in Southern Italy. Hydrol. Process. 24, 789–797.
Bautista, S., Mayor, A.G., Bourakhouadar, J., Bellot, J., 2007. Plant spatial pattern predicts hillslope runoff and erosion in a semiarid Mediterranean landscape. Ecosystems 10, 987–998.
Belnap, J., Welter, J.R., Grimm, N.B., Barger, N., Ludwig, J.A., 2005. Linkages between microbial and hydrologic processes in arid and semiarid watersheds. Ecology 86, 298–307.
Boix-Fayos, C., Martínez-Mena, M., Arnau-Rosalén, E., Calvo-Cases, A., Castillo, V., Albaladejo, J., 2006. Measuring soil erosion by field plots: understanding the sources of variation. Earth-Sci. Rev. 78, 267–285.
Bonta, J.V., 2000. Runoff-energy factors for MUSLE sediment-yield model for surface mines. Int. J. Sediment Res. 15, 162–181.
Cai, Q., Liu, J., Liu, Q., 2004. Research of sediment yield statistical model for single rainstorm in Chabagou drainage basin. Geogr. Res. 23, 433–439 in Chinese with English abstract.
Cammeraat, L.H., 2002. A review of two strongly contrasting geomorphological systems within the context of scale. Earth Surf. Process. Landf. 27, 1201–1222.
Cammeraat, E.L.H., 2004. Scale dependent thresholds in hydrological and erosion response of a semi-arid catchment in southeast Spain. Agric. Ecosyst. Environ. 104, 317–332.
Cerdà, A., Brazier, R., Nearing, M., de Vente, J., 2013. Scales and erosion. Catena 102, 1–2.
Chen, H., 2001. Relationship between erosion and sediment yield in drainage basins of loess gully-hilly areas. J. Geogr. Sci. 11, 71–79.
de Vente, J., Poesen, J., 2005. Predicting soil erosion and sediment yield at the basin scale: scale issues and semi-quantitative models. Earth-Sci. Rev. 71, 95–125.
de Vente, J., Poesen, J., Arabkhedri, M., Verstraeten, G., 2007. The sediment delivery problem revisited. Prog. Phys. Geogr. 31, 155–178.
de Vente, J., Poesen, J., Verstraeten, G., Govers, G., Vanmaercke, M., Van Rompaey, A., Arabkhedri, M., Boix-Fayos, C., 2013. Predicting soil erosion and sediment yield at regional scales: where do we stand? Earth-Sci. Rev. 127, 16–29.
Ellison, W.D., 1948. Soil Erosion. Soil Sci. Soc. Am. J. 12, 479–484.
Fang, H., Cai, Q., Chen, H., Huang, X., 2007a. Research on the dynamics of temporal sediment transport in a gullied Loess Basin: the Lower Chabagou Creek on the Loess Plateau. Prog. Geogr. 26, 77–87 in Chinese with English abstract.
Fang, H., Chen, H., Cai, Q., Huang, X., 2008. Effect of spatial scale on suspended sediment concentration in flood season in hilly loess region on the Loess Plateau in China. Environ. Geol. 54, 1261–1269.
Fang, H., Chen, H., Cai, Q., Li, Q., 2007b. Scale effect on sediment yield from sloping surfaces to basins in hilly loess region on the Loess Plateau in China. Environ. Geol. 52, 753–760.
Fang, H., Li, Q., Cai, Q., Liao, Y., 2011. Spatial scale dependence of sediment dynamics in a gullied rolling loess region on the Loess Plateau in China. Environ. Earth Sci. 64, 693–705.
Favis-Mortlock, D., Boardman, J., MacMillan, V., 2001. The limits of erosion modeling: why we should proceed with care. In: Harmon, R.S., Doe III, W.W. (Eds.), Landscape Erosion and Evolution Modeling. Kluwer Academic/Plenum Publishing, New York, pp. 477–516.
Ferguson, R.I., 1986. Hydraulics and hydraulic geometry. Prog. Phys. Geogr. 10, 1–31.
Foster, G.R., Lombardi, F., Moldenhauer, W.C., 1982. Evaluation of rainfall-runoff erosivity factors for individual storms. T. ASAE 25, 124–129.
Jetten, V., de Roo, A., Favis-Mortlock, D., 1999. Evaluation of field-scale and catchment-scale soil erosion models. Catena 37, 521–541.
Jetten, V., Govers, G., Hessel, R., 2003. Erosion models: quality of spatial predictions. Hydrol. Process. 17, 887–900.
Kinnell, P.I.A., 1997. Runoff ratio as a factor in the empirical modelling of soil erosion by individual rainstorms. Aust. J. Soil Res. 35, 1–13.
Kinnell, P.I.A., 2014. Applying the $Q_R EI_{30}$ index within the USLE modelling environment. Hydrol. Process. 28, 591–598.
Kirkby, M.J., Imeson, A.C., Bergkamp, G., Cammeraat, L.H., 1996. Scaling up processes and models from the field plot to the watershed and regional areas. J. Soil Water Conserv. 51, 391–396.
Knapen, A., Poesen, J., Govers, G., Gyssels, G., Nachtergaele, J., 2007. Resistance of soils to concentrated flow erosion: a review. Earth-Sci. Rev. 80, 75–109.
Knighton, A.D., 1999. Downstream variation in stream power. Geomorphology 29, 293–306.
Leopold, L.B., Maddock, T., 1953. The hydraulic geometry of stream channels and some physiographic implications. U. S. Geol. Surv. Prof. Pap. 252.
Li, Z., Li, P., Han, J., Li, M., 2009. Sediment flow behavior in agro-watersheds of the purple soil region in China under different storm types and spatial scales. Soil Tillage Res. 105, 285–291.
Liu, B.Y., Nearing, M.A., Shi, P.J., Jia, Z.W., 2000. Slope length effects on soil loss for steep slopes. Soil Sci. Soc. Am. J. 64, 1759–1763.
Mayor, Á.G., Bautista, S., Bellot, J., 2011. Scale-dependent variation in runoff and sediment yield in a semiarid Mediterranean catchment. J. Hydrol. 397, 128–135.
Meyer, L.D., Wischmeier, W.H., 1969. Mathematical simulation of the process of soil erosion by water. T. ASAE 12, 754–758 + 762.
Mu, J., Meng, Q., 1982. Sediment Delivery Ratio as Used in the Computation of the Watershed Sediment Yield. J. Sediment Res. 2, 223–230 (in Chinese).
Osterkamp, W.R., Toy, T.J., 1997. Geomorphic considerations for erosion prediction. Environ. Geol. 29, 152–157.
Parsons, A.J., Brazier, R.E., Wainwright, J., Powell, D.M., 2006. Scale relationships in hillslope runoff and erosion. Earth Surf. Process. Landf. 31, 1384–1393.
Parsons, A.J., Wainwright, J., Mark Powell, D., Kaduk, J., Brazier, R.E., 2004. A conceptual model for determining soil erosion by water. Earth Surf. Process. Landf. 29, 1293–1302.
Peters, D.P.C., Havstad, K.M., 2006. Nonlinear dynamics in arid and semi-arid systems: interactions among drivers and processes across scales. J. Arid Environ. 65, 196–206.
Puigdef Bregas, J., 2005. The role of vegetation patterns in structuring runoff and sediment fluxes in drylands. Earth Surf. Process. Landf. 30, 133–147.
Rodríguez-Blanco, M.L., Taboada-Castro, M.M., Taboada-Castro, M.T., 2013. Linking the field to the stream: soil erosion and sediment yield in a rural catchment, NW Spain. Catena 102, 74–81.
Roering, J.J., Kirchner, J.W., Dietrich, W.E., 1999. Evidence for nonlinear, diffusive sediment transport on hillslopes and implications for landscape morphology. Water Resour. Res. 35, 853–870.
Shu, A., Liu, Q., Yi, Y., Zhang, Z., 2008. Characteristics of energy dissipation in hyperconcentrated flows. Int. J. Sediment Res. 23, 387–397.
Singh, V.P., Zhang, L., 2008. At-a-station hydraulic geometry relations, 1: theoretical development. Hydrol. Process. 22, 189–215.
Vente, J., Verduyn, R., Verstraeten, G., Vanmaercke, M., Poesen, J., 2011. Factors controlling sediment yield at the catchment scale in NW Mediterranean geoecosystems. J. Soils Sediments 11, 690–707.
Wang, N.B., 1991. Dataset by Remote Sense for Resource and Environment in the Loess Plateau Region. Xi'an Press for Maps, Xi'an in Chinese.
Wilcox, B.P., Breshears, D.D., Allen, C.D., 2003. Ecohydrology of a resource-conserving semiarid woodland: effects of scale and disturbance. Ecol. Monogr. 73, 223–239.
Williams, J.R., Berndt, H.D., 1977. Sediment yield prediction based on watershed hydrology. T. ASAE 20, 1100–1104.

Xu, J., 1999. Erosion caused by hyperconcentrated flow on the Loess Plateau of China. Catena 36, 1–19.
Xu, J.X., 2004. Hyperconcentrated flows in the slope-channel systems in gullied hilly areas on the Loess Plateau, China. Geogr. Ann. 86A, 349–366.
Xu, J., Yan, Y., 2005. Scale effects on specific sediment yield in the Yellow River basin and geomorphological explanations. J. Hydrol. 307, 219–232.
Yellow River Conservancy Commission, Ministry of Water Conservancy and Electric Power, PRC, 1961–1971s. Obsewrved Data of Rainfall, Runoff and Sediment in the Zizhou Experimental Office over the Period 1959–1969 in Chinese.
Zheng, M., Chen, X., 2015. Statistical determination of rainfall-runoff erosivity indices for single storms in the Chinese Loess Plateau. PLoS One 10, e0117989.
Zheng, M., Cai, Q., Chen, H., 2007b. Effect of vegetation on runoff-sediment yield relationship at different spatial scales in hilly areas of the Loess Plateau, North China. Acta Ecol. Sin. 27, 3572–3581.
Zheng, M., Cai, Q., Cheng, Q., 2008. Modelling the runoff-sediment yield relationship using a proportional function in hilly areas of the Loess Plateau, North China. Geomorphology 93, 288–301.
Zheng, M., Cai, Q., Wang, C., Liu, J., 2007a. Effect of vegetation and other measures for soil and water conservation on runoff-sediment relationship in watershed scale. J. Hydraul. Eng. 38, 47–53 in Chinese with English abstract.
Zheng, M., Li, R., He, J., 2015. Sediment concentrations in run-off varying with spatial scale in an agricultural subwatershed of the Chinese Loess Plateau. Hydrol. Process. 29, 5414–5423.
Zheng, M., Qin, F., Sun, L., Qi, D., Cai, Q., 2011. Spatial scale effects on sediment concentration in runoff during flood events for hilly areas of the Loess Plateau, China. Earth Surf. Process. Landf. 36, 1499–1509.
Zheng, M., Qin, F., Yang, J., Cai, Q., 2013. The spatio-temporal invariability of sediment concentration and the flow-sediment relationship for hilly areas of the Chinese Loess Plateau. Catena 109, 164–176.
Zheng, M., Yang, J., Qi, D., Sun, L., Cai, Q., 2012. Flow-sediment relationship as functions of spatial and temporal scales in hilly areas of the Chinese Loess Plateau. Catena 98, 29–40.